Effects of anisotropic elasticity in the problem of domain formation and stability of monodomain state in ferroelectric films

A. M. Bratkovsky[1] and A. P. Levanyuk[1,2,3]

[1]*Hewlett-Packard Laboratories, 1501 Page Mill Road, Palo Alto, California 94304, USA*

[2]*Departamento de Física Teórica de la Materia Condensada, Universidad Autonoma de Madrid, Madrid E-28049, Spain*

[3]*Moscow Institute of Radioengineering, Electronics and Automation, Moscow 117454, Russia*

(Received 2 January 2011; revised manuscript received 13 March 2011; published 1 July 2011)

We study cubic ferroelectrics films that become uniaxial with a polar axis perpendicular to the film because of a misfit strain due to the substrate. The main present result is the analytical account for the elastic anisotropy as well as the anisotropy of the electrostriction. They define, in particular, the orientation of the domain boundaries and the stabilizing or destabilizing effect of inhomogeneous elastic strains on the single domain state. We apply the general results to perovskite systems like $BaTiO_3/SrRuO_3/SrTiO_3$ films and find that, at least not far from the ferroelectric phase transition, the equilibrium domain structure consists of the stripes along the cubic axes or at 45° to them. We also show that, in this system, the inhomogeneous strains increase stability with regard to small fluctuations of the metastable single domain state, which may exist not very close to the ferroelectric transition. The latter analytical result is in qualitative agreement with the numerical result by Pertsev and Kohlstedt [N. A. Pertsev and H. Kohlstedt, Phys. Rev. Lett. **98**, 257603 (2007)] but we show that the effect is much smaller than those authors claim. We find also that under some conditions on the material constants, which are not satisfied in perovskites but are not forbidden, in principle, instead of the striped-like domain structure a checkerboard one can be realized and the polarization-strain coupling decreases the stability of a single domain state instead of increasing it.

DOI: 10.1103/PhysRevB.84.045401 PACS number(s): 77.55.fe, 77.80.bn, 77.80.Dj

I. INTRODUCTION

The properties of domain structures in thin ferroelectric films are currently a focus of extensive research. It is expected that an understanding and an ability to control these properties will determine the prospects of applications of nanometer-sized ferroelectrics. It depends critically on the external conditions like the presence or absence of electrodes. In this paper, we discuss domain structures in a system, which are, perhaps, the most important for applications: a ferroelectric film with electrodes. The polar axis of the material is perpendicular to the film plane and the electrodes are "real," meaning that the electric field penetrates into them, although only over tiny depths <1 Å. This is an adequate model for the perovskite ferroelectric films on a substrate with a compressive strain, like $BaTiO_3/SrRuO_3/SrTiO_3$ (BTO/SRO/STO) (Refs. 1–5), where the misfit strain drives the ferroelectric (FE) film into a uniaxial state with a "soft" direction perpendicular to the plane. We supplement our analytical results with the relevant numerical estimates for $BaTiO_3$ (BTO), $PbTiO_3$ (PTO), and $Pb(Zr_{0.5}Ti_{0.5})O_3$ (PZT) using the material constants available in the literature.

We shall be interested in properties of the domain structure close to the phase transition from the paraelectric phase, either by lowering temperature at a constant film thickness or by increasing the film thickness at constant temperature. It is worth mentioning that most theoretical papers are concerned with the domain structure far from the phase transition (see, e.g., the references in Ref. 6). The approximations made within this approach are not valid near the phase transition from the paraelectric phase and there are two ways to overcome this difficulty. One, by brute force numerical calculation, was recently pursued by Stephenson and Elder[7] who went beyond the standard ("linear") approximation by explicitly taking into account nonlinear and nonlocal terms in the constituent equations. They also simplified the elastic part of the problem by assuming that the strains associated with the inhomogeneous ferroelectric polarization are homogeneous over the film volume. Another way to consider the vicinity of the phase transition was proposed long ago by Suhl,[8] Schmidt *et al.*,[9] and Chensky and Tarasenko,[10] whose starting point was solving the problem of *stability* of the paraelectric phase which gives the phase transition temperature (the critical film thickness) and the form of the inhomogeneous polarization distribution with respect to which the stability is lost. This part of the problem involves the solution of a system of *linear* differential equations that can be made exactly, without any approximation. But the information obtained at this stage is not sufficient for a complete description of the domain structure in the ferroelectric phase. It is natural to expect that the form of the inhomogeneous polarization distribution found from the stability problem also has the functional form of this distribution in the ferroelectric phase close to the phase transition, but the problem is that the linear problem of the stability loss provides the form only, not the amplitude. This can be found by taking into account the nonlinear terms, which is possible within an approximation: The form of the inhomogeneous polarization distribution in the ferroelectric phase is, of course, different far and close to the transition, but it is similar to the one obtained from the solution of the linear problem close enough to the phase transition. The region where this ("one sinusoid") approximation is valid is broader the less the film thickness is and for films of tens of nanometers thickness, which we are interested in, can be quite broad.[7]

We shall use this approximation because it allows to take into account explicitly and within analytical calculations the

inhomogeneities of the polarization-induced elastic strains that appeared to be too difficult even for numerical calculations within the method used in Ref. 7. This account is necessary for revealing some important features of the domain structure, specifically, to find out if the equilibrium structure is a stripe-like or a checkerboard one and how the domain boundaries are oriented with respect to the crystallographic axes. This is the main goal of the present paper. Specifically, we consider the case of cubic crystal anisotropy of elastic and electrostrictive properties only. This is relevant for films of cubic perovskites which become tetragonal as a result of in-plane misfit compressive strains due to cubic substrates like in the above-mentioned system. The changeover from cubic to tetragonal anisotropy affects most strongly the dielectric properties since the crystals are "soft" dielectrically. They have a much smaller effect on the elastic and electrostrictive properties, which can be considered to be the same as in the cubic parent crystals. Importantly, the formation of the domain structure at the phase transition takes place in our case because of the incomplete screening of the depolarizing field by the real electrode (e.g., by the $SrRuO_3$ electrode in the BTO/SRO/STO system.[5,6,11])

It seems that this situation is typical of real electrodes and we shall consider this case only. In this situation, the single domain state appears to be absolutely unstable just below the transition. The presence of the electrode has its effect that farther from the phase transition the single domain state becomes metastable instead of being absolutely unstable.[6] To find the temperature or the film thickness corresponding to this change (i.e., to find the limit of the metastability of the single domain state) one has to take into account the inhomogeneous strains accompanying the inhomogeneous polarization. This has been correctly pointed out by Pertsev and Kohlstedt[12–14] although these authors missed several important points.[15] Here, we only mention that they performed numerical calculations for a specific system, but made a general statement about the stabilization of single domain states due to the coupling of inhomogeneous polarization with inhomogeneous elastic strains. Our analytical treatment shows that as a general physical phenomenon such a stabilization does *not* exist and the polarization-strain coupling can have, in principle, both stabilizing and destabilizing effects if a certain condition on the electrostrictive and elastic constants is met. We are not aware of an experimental realization of these conditions, but we cannot find arguments prohibiting them. It is worth mentioning that a qualitative conclusion about the possibility of both the stabilizing and destabilizing role of inhomogeneous elastic strains for a single domain state in ferroelectric films on substrates has been made in our previous paper where we considered an academic case of a single electrostriction constant and assumed isotropic elasticity.[16] A surprising result of the present work is that the *destabilizing* effect of the inhomogeneous strains may be very large, contrary to the stabilizing one. For perovskites, this coupling has indeed a stabilizing effect though it is much more modest compared to what was claimed in Ref. 13.

Studying the sinusoidal domain structure in BTO, PTO, and PZT films on $SrTiO_3$, we find that the equilibrium orientation of the "domain walls" is parallel (perpendicular) to the cubic axes in the film plane for BTO and PTO and is at 45° to these axes for PZT. In all cases, the free energy of the sinusoidal domain structure depends very weakly on the domain wall orientation. This is mainly due to both systems being nearly isotropic elastically and, additionally, the relevant electrostriction constant is relatively small. This observation may be important for understanding domain creation at the smallest thicknesses of the ferroelectric films. Another unexpected result is the possibility of a checkerboard domain state if some conditions on the materials constants are met. Let us mention that without accounting for the anisotropic polarization-strain coupling such a state is impossible. This conclusion remains valid for the perovskites, but not in the general case.

Having indicated the advantages and new possibilities provided by analytical calculations, we should mention also their inherent shortcomings. Our analytical method is feasible within a certain approximation only. This approximation implies that the domain period is less than the film thickness. This condition is fulfilled for thick enough films, but in very thin films the two quantities are, in fact, comparable. Therefore, the accuracy of our calculations should be investigated for these films, so the new numerical studies are desirable. We do not expect, however, that the difference between the results of the approximated and more exact calculations either within a continuous medium theory or within microscopic theories will be very large given the close results of continuous and first principles theories even for films that are just several unit cell thick (see e.g., Ref. 11).

The paper is organized as follows. We describe the approximations used and define the terms in the Landau-Ginzburg-Devonshire (LGD) free energy that can be neglected within our approximation in Sec. II. This lets us avoid unnecessary, lengthy formulas in the rest of the paper. We spell out the constituent equations in Sec. III and then solve the general problem for the "polarization wave" (embryonic stripe domains) in the FE film with a full account for the elastic coupling. This is further used in Sec. V to determine how the domain walls align with the crystallographic cubic axes in thermodynamic equilibrium. Then, we find the conditions when the monodomain state loses its stability with regard to the stripe domain structure in Sec. VI. One previously unexplored possibility is that the system can lose stability with regard to the checkerboard domain structure, but our results in Sec. VII show that such a structure is absolutely unstable in perovskites although it is not necessarily so in the general case. We summarize the present results in the Conclusion.

II. OUTLINE OF THE METHOD AND THE APPROXIMATIONS USED

The main conclusions of this paper are made by analyzing the formula for the free energy of the total system as a function of the amplitude a of the ferroelectric "polarization wave" presenting the sinusoidal domain structure and the homogeneous part of the ferroelectric polarization, p. For the electrode and the film parameters of a system like BTO/SRO/STO, the ferroelectric polarization that is perpendicular to the film plane, a schematic of which is shown in Fig. 1, has the form

$$P_z(x,y,z) = p + a\cos \boldsymbol{kr}\cos qz, \tag{1}$$

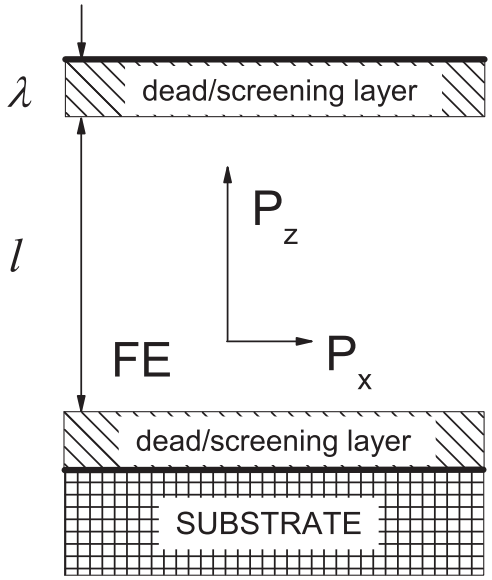

FIG. 1. Schematic of the (perovskite) ferroelectric film with thickness l and metal electrodes (with screening length λ) on a misfit substrate. The misfit makes the film a uniaxial ferroelectric with a spontaneous polarization along the z axis.

where the orientation of $\boldsymbol{k}$ in the x,y plane is not fixed, $2\pi/k$ is the period of the sinusoidal domain structure $q = \pi/l$, and l is the film thickness. To find the desired free energy, $F(a,p)$, one has to find the elastic strains and the nonferroelectric polarization $\boldsymbol{P}_\perp = (P_x, P_y)$ as functions of a and p to present the total free energy as a function of a and p only. The total free energy contains contributions of the ferroelectric film, of the substrate, and of the electrode. In principle, it should also contain a contribution of the voltage source, but we consider here a *short-circuited* system and are not concerned with this last contribution.

When calculating elastic strains in the ferroelectric, which accompany the inhomogeneous polarization forming the sinusoidal domain structure, we follow the same philosophy as in our previous work.[16] In principle, when calculating these strains the inhomogeneous strains in the substrate should be taken into account. However, it is well known that they propagate into the substrate for about the same distances as the scale of inhomogeneity (domain width) in the film (x,y) plane. In our case, these inhomogeneities are due to the domain structure (i.e., this scale is the period of the domain structure). Then, it is convenient to consider relatively thick films since the period of the domain structure is relatively small, specifically, it is much less than the film thickness,[6,10] Fig. 2. The contribution of the substrate is its elastic energy, which, as we have mentioned above, is concentrated within a volume that is *much smaller* than the film volume, as defined by a small factor $q/k = \pi/kl \ll 1$. Another convenience of the thick film limit is that it is possible to disregard the boundary conditions for the inhomogeneous parts of the elastic strains and stresses at the surfaces of the ferroelectric. Indeed, if we obtain a solution which does not satisfy the boundary conditions, we can find corrections to such a solution in a way that is customarily used in the elasticity theory (see e.g., Refs. 18 and 19). First, we apply the external forces to the

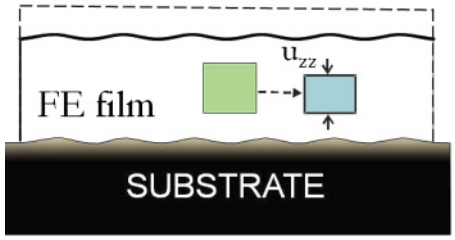

FIG. 2. (Color online) Schematic of the ferroelectric film on the misfit substrate at the onset of sinusoidal polarization wave. The elastic coupling to the substrate allows inhomogeneous deformations, but prohibits homogeneous strains in the plane of the film.

surfaces, which are necessary to meet the boundary conditions with the strains corresponding to our solution making this solution correct. Second, we apply forces opposite to the previous ones and find the strains produced by the new forces. These strains provide the correction to the original solution we were looking for. Once more, it is sufficient to observe that in our case the external forces have the period of the domain structure to understand that the elastic energy associated with the corrections necessary to satisfy the boundary conditions can be neglected quite similarly to the elastic energy of the substrate. This is equivalent to the arguments of Refs. 19 and 16 made in a similar context.

Another convenience of the thick film approximation is given by the possibility to neglect those terms in the LGD free energy, which describes the electrostriction but contains components of a nonferroelectric polarization. According to Refs. 6 and 10,

$$\boldsymbol{P}_\perp(x,y,z) = (\boldsymbol{k}/k)a_\perp \sin \boldsymbol{kr} \sin qz, \tag{2}$$

where $a_\perp \approx aq/k$, $q/k = \pi/kl \ll 1$. The electrostriction terms in the LGD free energy with nonferroelectric components of polarization may contain the ferroelectric component, like $P_x P_z u_{xz}$, or may not contain them, like in the term $P_x P_y u_{xy}$. In both cases, they contribute to the a^4 and p^2a^2 terms in the free energy depending on a and p. In the first case, this contribution is proportional to $(q/k)^2$ and in the second to $(q/k)^4$. Since there are also the terms a^4, p^2a^2 that do not contain the small factor q/k, the contribution of these terms can be neglected.

Taking this into account, we write down the LGD free energy density in the form

$$F(\boldsymbol{P},u_{ik}) = F_1(\boldsymbol{P}) + F_2(u_{ik}) + F_3(\boldsymbol{P},u_{ik}), \tag{3}$$

where

$$F_1(\boldsymbol{P}) = \frac{A}{2}P_z^2 + \frac{B}{4}P_z^4 + \frac{1}{2}G(\nabla_\perp P_z)^2 + \frac{1}{2}\kappa P_{bz}^2 + \frac{A_\perp}{2}P_\perp^2, \tag{4}$$

$$F_2(u_{ik}) = \tfrac{1}{2}\lambda_1\left(u_{xx}^2 + u_{yy}^2 + u_{zz}^2\right) + \lambda_2(u_{xx}u_{yy} + u_{xx}u_{zz} + u_{zz}u_{yy}) + 2\mu\left(u_{xy}^2 + u_{zy}^2 + u_{xz}^2\right), \tag{5}$$

$$F_3(\boldsymbol{P},u_{ik}) = q_{11}u_{zz}P_z^2 + q_{12}(u_{xx} + u_{yy})P_z^2. \tag{6}$$

Here, $q_{11(12)}$ are the standard piezoelectric coefficients that should not be confused with the parameter q defining the transversal profile of the polarization wave (1). In Eq. (4),

$A = \gamma(T - T_c)$, $B, G = \text{const}$, $\vec{\nabla}_\perp = (\partial_x, \partial_y)$ the gradient in the plane of the film P_{bz} is the nonferroelectric ("base") part of the polarization perpendicular to the electrodes,[17] $A_\perp > 0$. We have neglected higher terms in $P_\perp$ because of the smallness of these components as it follows from Eq. (2). Following Refs. 6 and 10, we have neglected a term with the gradient in z direction since it is much smaller than the one in the plane of the film, which one can write formally as a condition $\partial_z \ll \vec{\nabla}_\perp$. It is worth mentioning that we have not included the energy of the electric field into the LGD free energy. The reason is that we shall use it to write down the constituent equations only. We shall eliminate u_{ik}, $\boldsymbol{P}_\perp$, P_{bz} as well the electric field components from the system of constituent and electrostatics equations to obtain two coupled equations of state for a and p. We shall obtain $F(p,a)$ from the resulting equations. This is possible because of the thick films approximation. The most straightforward method to obtain $F(p,a)$ would be to substitute Eq. (1) into Eq. (3), supplemented by the electric field energy and to integrate over the film volume. In general, the result would not be the same as the one obtained from the constituent equations because of the approximate character of Eq. (1). However, for $q = \pi/l$ the two results coincide and that makes it possible to use a more convenient method of the constituent equations.

III. CONSTITUENT EQUATIONS

For the polarization components one has

$$A P_z + B P_z^3 - G \nabla_\perp^2 P_z + 2q_{11} P_z u_{zz} + 2q_{12} P_z (u_{xx} + u_{yy}) = E_z, \tag{7}$$

$$P_{bz} = \kappa E_z, \tag{8}$$

$$\boldsymbol{P}_\perp = A_\perp \boldsymbol{E}_\perp. \tag{9}$$

Before writing down the equations for the strain, we shall eliminate the electric field from the above three equations. Assuming Eq. (1) for P_z, Eq. (2) for $\boldsymbol{P}_\perp$, and putting[6]

$$E_{0z} = E_0 + E_z^k \cos \boldsymbol{kr} \cos qz, \qquad \boldsymbol{E}_\perp = (\boldsymbol{k}/k) E_\perp^k \sin \boldsymbol{kr} \sin qz, \tag{10}$$

we can replace Eqs. (7) and (9) with

$$Ap + \left[B P_z^3 + 2q_{11} P_z u_{zz} + 2q_{12} P_z u_{\perp\perp}\right]_{\text{hom}} = E_0, \tag{11}$$

$$(A + Gk^2)a + \left[B P_z^3 + 2q_{11} P_z u_{zz} + 2q_{12} P_z u_{\perp\perp}\right]_{\text{cc}} = E_z^k, \tag{12}$$

$$A_\perp a_\perp = E_\perp^k, \tag{13}$$

where $u_{\perp\perp} = u_{xx} + u_{yy}$, $[\cdots]_{\text{hom}}$ and $[\cdots]_{\text{cc}}$ denote the homogeneous part ($k = 0$) and the part proportional to $\cos \boldsymbol{kr} \cos qz$ of the expression in the brackets, correspondingly. Of course, as a result of this replacement, a part of the left-hand side (l.h.s.) of Eq. (7) is lost, but it corresponds to the higher harmonics of the sinusoidal distribution of the polarization and these harmonics can be neglected close to the transition.[6,10]

The homogeneous part of the electric field E_{0z} can be calculated as, for example, in Ref. 6 yielding for the short-circuited case

$$E_{0z} = -\frac{4\pi d}{\varepsilon_b d + \epsilon_e l} p, \tag{14}$$

where d is the thickness of the dead layer and ϵ_e its dielectric constant. Recall that real electrodes have finite, albeit small (Thomas-Fermi) screening length λ, which is completely analogous[6] to the presence of the "dead" nonferroelectric layers at the interface with thickness $d/2 = \lambda$. Using Eqs. (14), (11) gets the form

$$A_1 p + \left[B P_z^3 + 2q_{11} P_z u_{zz} + 2q_{12} P_z (u_{xx} + u_{yy})\right]_{\text{hom}} = 0, \tag{15}$$

where

$$A_1 = A + \frac{4\pi d}{\varepsilon_b d + \epsilon_e l} \approx A + \frac{4\pi d}{\epsilon_e l}, \tag{16}$$

since usually the dead layer is very thin, $\varepsilon_b d \ll \epsilon_e l$. To transform Eq. (12) we use the electrostatics equation

$$\text{div} \boldsymbol{D} = 0, \tag{17}$$

where $\mathbf{D}$ is the dielectric displacement. For the ferroelectric material, taking into account that $\boldsymbol{D} = (\varepsilon_\perp \boldsymbol{E}_\perp, \ \varepsilon_b E_z + 4\pi P_z)$, where $\varepsilon_\perp = 1 + 4\pi/A_\perp$, and $\varepsilon_b = 1 + 4\pi/\kappa$ is the *base* noncritical dielectric constant,[6,17] and together with the equation curl $\boldsymbol{E} = 0$, we find that

$$E_z^k = -\frac{4\pi q^2}{\varepsilon_\perp k^2} a. \tag{18}$$

Using this expression for the field E_z^k, we can rewrite Eq. (12) as the homogeneous one

$$[A + Gk^2 + 4\pi q^2/(\varepsilon_\perp k^2)]a + \left[B P_z^3 + 2q_{11} P_z u_{zz} + 2q_{12} P_z u_{\perp\perp}\right]_{\text{cc}} = 0. \tag{19}$$

The transition takes place when the first coefficient in square brackets goes negative for the first time upon lowering temperature through some $T = T_d$, namely, when (recall that $A \propto T - T_c$)

$$-A \equiv -A(T_d) = [Gk^2 + 4\pi q^2/(\varepsilon_\perp k^2)]_{\text{min}}.$$

This takes place at the wave vector k satisfying the condition (recall that $q = \pi/l$)

$$\frac{4\pi q^2}{\varepsilon_\perp k^2} = Gk^2, \quad k = \left(\frac{4\pi q^2}{\varepsilon_\perp G}\right)^{1/4}, \tag{20}$$

we rewrite Eq. (12) as the homogeneous one

$$A_2 a + \left[B P_z^3 + 2q_{11} P_z u_{zz} + 2q_{12} P_z u_{\perp\perp}\right]_{\text{cc}} = 0, \tag{21}$$

where

$$A_2 = A + 2Gk^2. \tag{22}$$

It is seen from Eq. (6) that the only source of elastic stresses and strains is $P_z^2(x,y,z)$ in our approximation. Since

$$P_z^2 = p^2 + 2pa \cos \boldsymbol{kr} \cos qz + \frac{a^2}{4}(1 + \cos 2qz + \cos 2\boldsymbol{kr} + \cos 2\boldsymbol{kr} \cos 2qz), \tag{23}$$

we should expect that

$$u_{zz} = u_{zz}^{(0)} + u_{zz}^{(1)} \cos 2qz + u_{zz}^{(2)} \cos \boldsymbol{kr} \cos qz + u_{zz}^{(3)} \cos 2\boldsymbol{kr} + u_{zz}^{(4)} \cos 2\boldsymbol{kr} \cos 2qz, \quad (24)$$

while for u_{xx}, u_{yy}, and for $u_{\perp\perp}$ we shall have similar formulas with the homogeneous part (first term in the above expression) absent because of the substrate. The superscripts (0)–(4) denote contributions with different types of the coordinate dependencies as defined by Eq. (24). Below, we use the same superscripts for both the coefficients and the functions.

Substituting Eqs. (23) and (24), and analogous equations for u_{xx} and u_{yy} into Eqs. (15) and (21), we find

$$A_1 p + \left[B P_z^3\right]_{\text{hom}} + 2q_{11}\left(p u_{zz}^{(0)} + \frac{a u_{zz}^{(2)}}{4}\right) + q_{12}\frac{a}{2} u_{\perp\perp}^{(2)} = 0, \quad (25)$$

$$A_2 a + \left[B P_z^3\right]_{\text{cc}} + 2q_{11}\left[p u_{zz}^{(2)} + a\left(u_{zz}^{(0)} + \frac{u_{zz}^{(1)} + u_{zz}^{(3)}}{2} + \frac{u_{zz}^{(4)}}{4}\right)\right] + 2q_{12}\left[p u_{\perp\perp}^{(2)} + a\left(\frac{u_{\perp\perp}^{(1)} + u_{\perp\perp}^{(3)}}{2} + \frac{u_{\perp\perp}^{(4)}}{4}\right)\right] = 0. \quad (26)$$

We shall calculate the values $u_{ik}^{(j)}$ in the next section by solving the elastic problem explicitly.

Importantly, the above equation of state (25) suggests that the film would tend to transform into a single domain (SD) state with $p \neq 0$ and $a = 0$ at temperature T_c^{SD} such that $A_1 = 0$ or, in other words,

$$A\left(T_c^{\text{SD}}\right) = -4\pi d/(\epsilon_e l). \quad (27)$$

The second equation of state (26) yields a transition into a domain state ($p = 0$ and $a \neq 0$) at the temperature T_d such that $A_2 = 0$, or

$$A(T_d) = -2Gk^2. \quad (28)$$

Recall that in the present case, corresponding to $BaTiO_3/SrRuO_3/SrTiO_3$ (Ref. 5),

$$\frac{4\pi d}{\epsilon_e l} > 2Gk^2 \sim \frac{4\pi d_{at}}{\varepsilon_\perp^{1/2} l}, \quad (29)$$

where $d_{at} = \sqrt{\pi G} \approx 1$ Å is the small "atomic" length scale [$G = 0.3$ Å^2 for $BaTiO_3$ (Refs. 5 and 6)]. The above relation means that the paraphase gives way to the *domain phase*, with $a \neq 0$, thus preventing it from reaching the temperature T_c^{SD} where it could have transformed into a single domain state. Obviously, the same is true of the phase transformations in the film as a function of *thickness* at constant temperature. There, one can introduce the critical thickness for domains l_d, where

$$A(l_d) = -2Gk^2, \quad (30)$$

and the "critical thickness for the single domain state" l_c^{SD}, such that

$$A\left(l_c^{\text{SD}}\right) = -4\pi d/\left(\epsilon_e l_c^{\text{SD}}\right). \quad (31)$$

These introduced critical thicknesses and temperatures are discussed in detail below in Sec. VI.

IV. ELASTIC PROBLEM

Using Eqs. (5) and (6), we obtain for the diagonal components of the elastic stress tensor

$$\sigma_{xx} = \lambda_1 u_{xx} + \lambda_2(u_{yy} + u_{zz}) + q_{12} P_z^2, \quad (32)$$

$$\sigma_{yy} = \lambda_1 u_{yy} + \lambda_2(u_{xx} + u_{zz}) + q_{12} P_z^2, \quad (33)$$

$$\sigma_{zz} = \lambda_1 u_{zz} + \lambda_2(u_{xx} + u_{yy}) + q_{11} P_z^2, \quad (34)$$

and formulas of the type

$$\sigma_{xy} = 2\mu u_{xy}, \quad (35)$$

for the off-diagonal components.

We have already mentioned that the only u_{ik} component which has a part is u_{zz}. This part is easily found from the condition at the free surface $\sigma_{zz} = 0$ at $z = l/2$. From Eq. (34), one finds

$$u_{zz}^{(0)} = -\frac{q_{11}}{\lambda_1}\left[P_z^2\right]_{\text{hom}} = -\frac{q_{11}}{\lambda_1}\left(p^2 + \frac{a^2}{4}\right). \quad (36)$$

For the parts depending on z *only*, the equations of elastic equilibrium take the form

$$\partial \sigma_{iz}^{(1)}/\partial z = 0, \quad (37)$$

that is, $\sigma_{iz}^{(1)} = \text{const} = 0$ since it should vanish at the free surface ($z = l/2$). Therefore, Eqs. (34) and (23) yield

$$u_{zz}^{(1)} = -q_{11} a^2/(4\lambda_1), \quad (38)$$

and

$$u_{xx}^{(1)} = u_{yy}^{(1)} = 0, \quad (39)$$

because of the Saint-Venant's elastic compatibility conditions for z-only dependent strains.

When solving the rest of the elastic problem, we shall use the small parameter $q/k \ll 1$. This allows us to neglect the derivatives with respect to z: formally, $\partial/\partial z \ll \partial/\partial x, \partial/\partial y$. As a result, the equations of the elastic equilibrium acquire the form

$$\frac{\partial \sigma_{xx}^{(2-4)}}{\partial x} + \frac{\partial \sigma_{xy}^{(2-4)}}{\partial y} = \frac{\partial \sigma_{yz}^{(2-4)}}{\partial y} + \frac{\partial \sigma_{zx}^{(2-4)}}{\partial x} = \frac{\partial \sigma_{yy}^{(2-4)}}{\partial y} + \frac{\partial \sigma_{yx}^{(2-4)}}{\partial x} = 0, \quad (40)$$

where the superscripts (2–4) denote the part of the stresses that are due to the three last terms in Eq. (23), which we denote as $P_z^{2(2-4)}$. Explicitly,

$$\lambda_1 \frac{\partial^2 u_x^{(2-4)}}{\partial x^2} + \lambda_2 \frac{\partial^2 u_y^{(2-4)}}{\partial y \partial x} + \mu \frac{\partial^2 u_x^{(2-4)}}{\partial y^2} + \mu \frac{\partial^2 u_y^{(2-4)}}{\partial y \partial x} + q_{12} \frac{\partial P_z^{2(2-4)}}{\partial x} = 0, \quad (41)$$

$$\mu \frac{\partial^2 u_z^{(2-4)}}{\partial y^2} + \mu \frac{\partial^2 u_z^{(2-4)}}{\partial x^2} = 0, \quad (42)$$

$$\lambda_1\frac{\partial^2 u_y^{(2-4)}}{\partial y^2}+\lambda_2\frac{\partial^2 u_x^{(2-4)}}{\partial y\partial x}+\mu\frac{\partial u_x^{(2-4)}}{\partial x\partial y}+\mu\frac{\partial^2 u_y^{(2-4)}}{\partial x^2}+q_{12}\frac{\partial P_z^{2(2-4)}}{\partial y}=0. \quad (43)$$

Analogously to the isotropic case[16], we shall put the conditions $u_z^{(2-4)}=0$ that satisfy Eq. (42), but not, of course, the boundary conditions. They are not important in our approximation, as we argued above. Therefore, we conclude that

$$u_{zz}^{(2)}=u_{zz}^{(3)}=u_{zz}^{(4)}=0, \quad (44)$$

and we are left with only two equations to solve. It is convenient to solve them separately for (2) and (3,4) parts, since they correspond to different spatial harmonics.

Simplifying the remaining equations (41) and (43), we obtain

$$\lambda_1\frac{\partial^2 u_x^{(2-4)}}{\partial x^2}+(\lambda_2+\mu)\frac{\partial^2 u_y^{(2-4)}}{\partial y\partial x}+\mu\frac{\partial^2 u_x^{(2-4)}}{\partial y^2}+q_{12}\frac{\partial P_z^{2(2-4)}}{\partial x}=0, \quad (45)$$

$$\lambda_1\frac{\partial^2 u_y^{(2-4)}}{\partial y^2}+(\lambda_2+\mu)\frac{\partial^2 u_x^{(2-4)}}{\partial y\partial x}+\mu\frac{\partial^2 u_y^{(2-4)}}{\partial x^2}+q_{12}\frac{\partial P_z^{2(2-4)}}{\partial y}=0. \quad (46)$$

For the terms $u^{(2)}$, we have $P_z^{2(2)}\propto\cos\boldsymbol{kr}, \partial_{x(y)}P_z^2\propto -k_{x(y)}\sin\boldsymbol{kr}$, meaning that $u_{x(y)}\propto\sin\boldsymbol{kr}$, $\partial^2 u_i/\partial x^2=-k_x^2 u_i$, and so on. Then,

$$\lambda_1 k_x^2 u_x^{(2)}+(\lambda_2+\mu)k_x k_y u_y^{(2)}+\mu k_y^2 u_x^{(2)}+q_{12}k_x 2pa=0, \quad (47)$$

$$\lambda_1 k_y^2 u_y^{(2)}+(\lambda_2+\mu)k_x k_y u_x^{(2)}+\mu k_x^2 u_y^{(2)}+q_{12}k_y 2pa=0. \quad (48)$$

The terms $u^{(3),(4)}$ correspond to higher spatial harmonics in Eq. (23), but they should be taken into account since they contribute to the terms with the main harmonic in the constituent equation (26). Since for this part $P_z^2\propto\cos 2\boldsymbol{kr}$, we obtain a slightly different set of equations

$$\lambda_1 k_x^2 u_x^{(3,4)}+(\lambda_2+\mu)k_x k_y u_y^{(3,4)}+\mu k_y^2 u_x^{(3,4)}+q_{12}k_x\frac{a^2}{8}=0, \quad (49)$$

$$\lambda_1 k_y^2 u_y^{(3,4)}+(\lambda_2+\mu)k_x k_y u_x^{(3,4)}+\mu k_x^2 u_y^{(3,4)}+q_{12}k_y\frac{a^2}{8}=0. \quad (50)$$

Note that for the constituent equations we need the combinations

$$u_{\perp\perp}^{(2)}=u_{xx}^{(2)}+u_{yy}^{(2)}=k_x u_x^{(2)}+k_y u_y^{(2)},$$
$$u_{\perp\perp}^{(3,4)}=u_{xx}^{(3,4)}+u_{yy}^{(3,4)}=2k_x u_x^{(3,4)}+2k_y u_y^{(3,4)}.$$

We find

$$u_{\perp\perp}^{(2)}=-2q_{12}apf(\theta), \quad (51)$$

where θ is defined by $k_x=k\cos\theta$, $k_y=k\sin\theta$, and the function $f(\theta)$ is

$$f(\theta)=2\frac{(\lambda_1-\lambda_2)\sin^2 2\theta+2\mu\cos^2 2\theta}{(\lambda_1+\lambda_2+2\mu)(\lambda_1-\lambda_2)\sin^2 2\theta+4\lambda_1\mu\cos^2 2\theta}. \quad (52)$$

For terms, corresponding to $\cos 2\boldsymbol{kr}$ and $\cos 2qz$, we obtain

$$u_{\perp\perp}^{(3)}=u_{\perp\perp}^{(4)}=-q_{12}\frac{a^2}{4}f(\theta). \quad (53)$$

Using the results of the solution of the elastic problem, Eqs. (36), (44), (51) and (53), we can write Eqs. (25) and (26) as

$$A_1 p+\left(B-\frac{2q_{11}^2}{\lambda_1}\right)p^3+pa^2\frac{3}{4}\left[B-\frac{4}{3}\left(\frac{q_{11}^2}{2\lambda_1}q_{12}^2 f(\theta)\right)\right]=0, \quad (54)$$

$$A_2 a+a^3\frac{9}{16}\left(B-\frac{4}{3}\left[\frac{q_{11}^2}{\lambda_1}+\frac{q_{12}^2}{2}f(\theta)\right]\right)+ap^2 3\left(B-\frac{4}{3}\left[\frac{q_{11}^2}{2\lambda_1}+q_{12}^2 f(\theta)\right]\right)=0. \quad (55)$$

From these two constituent equations corresponding to an extremum of the free energy, one can easily reconstruct the free energy $\tilde{F}(p,a)$

$$V^{-1}\tilde{F}(p,a)=\frac{A_1}{2}p^2+\frac{A_2}{8}a^2+\frac{\widetilde{B}}{4}p^4+\frac{3B_1(\theta)}{8}a^2p^2\frac{9B_2(\theta)}{256}a^4, \quad (56)$$

where V is the FE film volume and

$$\widetilde{B}=B-\frac{2q_{11}^2}{\lambda_1},\quad B_1(\theta)=\widetilde{B}+\frac{4}{3}\left[\frac{q_{11}^2}{\lambda_1}-q_{12}^2 f(\theta)\right],\quad B_2(\theta)=\widetilde{B}+\frac{2}{3}\left[\frac{q_{11}^2}{\lambda_1}-q_{12}^2 f(\theta)\right], \quad (57)$$

are the Landau coefficients before the quartic terms renormalized by the strain. The form of the free energy is the same as in the isotropic case,[6,10,16] but, importantly, the coefficients B_1 and B_2 depend on the *orientation* of the "polarization wave" given by the angle θ.

V. ORIENTATION OF THE DOMAIN STRUCTURE

Consider the domain structure formed close to the paraelectric-ferroelectric transition. Although the stability of the paraelectric phase is lost with respect to the polarization waves with the value of the $\boldsymbol{k}$ vector given by Eq. (20) and arbitrary orientation in the x-y plane (i.e., for any θ) the energy of the sinusoidal domain structure depends on θ and one has to find the ones corresponding to the equilibrium domain structure(s). Since we consider here one "polarization wave" only, we study the competition between the stripe-type structures. In Sec. VII we shall show that the square (checkerboard) domain structure is unstable in perovskite crystals that we study here. The checkerboard structure could, in principle, be stable or metastable under some conditions

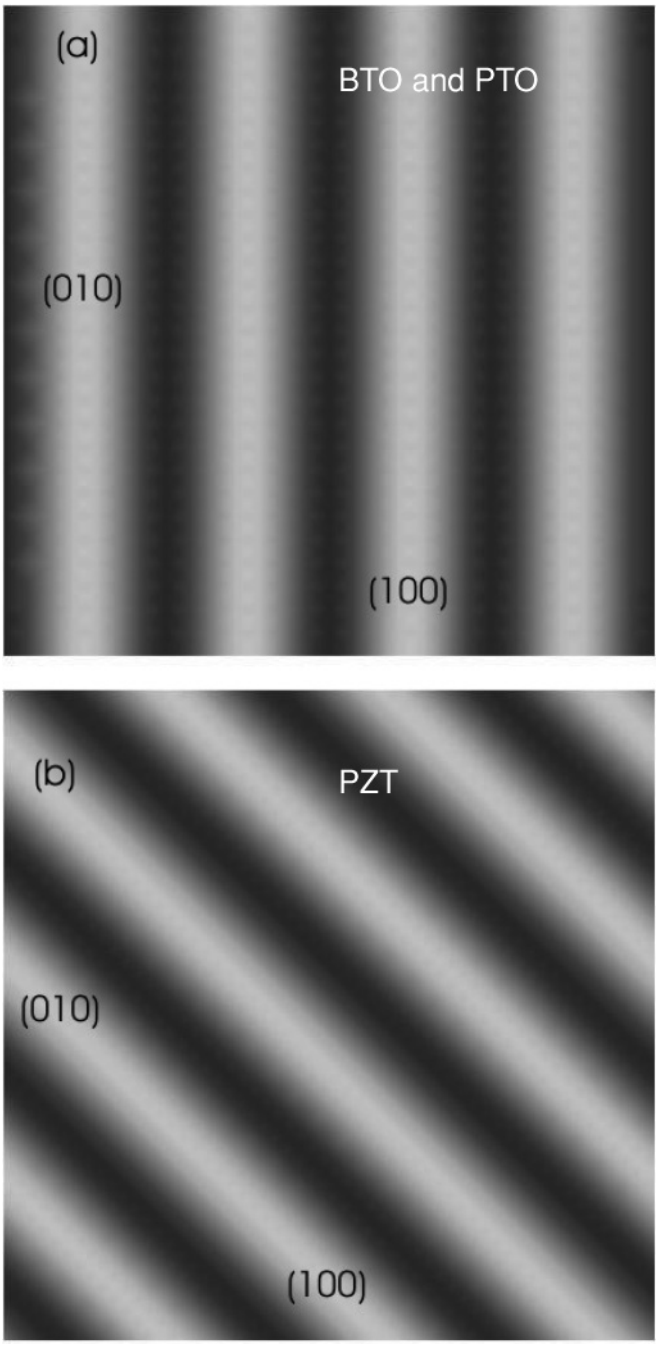

FIG. 3. Schematic of the sinusoidal domain structure in (a) BTO and PTO and (b) PZT. While the stripes are oriented along the crystal axes in case (a), in case (b) the stripes are at 45 degrees with respect to cubic axes, the difference being due to an opposite sign of elastic anisotropy in those two cases.

on the material constants, but we are not aware of any experimental example of this type, so it will be premature to study such a hypothetical case.

Recall that we discuss the ferroelectric phase transition in a sample with short-circuited electrodes. Then, $p = 0$ in the ferroelectric phase at least not far from the phase transition, and the phase transition into the inhomogeneous domain phase occurs at $A_2 = 0$. The free energy is

$$V^{-1}\tilde{F}(p,a) = \frac{A_2}{8}a^2 + \frac{9B_2(\theta)}{256}a^4. \tag{58}$$

At a fixed θ, the minimum of this free energy is realized for

$$a^2 = -\frac{16A_2}{9B_2(\theta)}, \tag{59}$$

with the corresponding free energy

$$V^{-1}\tilde{F}_{\min}(p,a) = -\frac{A_2^2}{9B_2(\theta)}. \tag{60}$$

We see that the equilibrium domain structure is realized for the angles θ which minimize the function $B_2(\theta)$ or, according to Eq. (57), *maximize* the function $f(\theta)$. Let us find the maxima of this function. It can be written in the form

$$f(\theta) = \frac{2}{\lambda_1 + \lambda_2 + 2\mu}\left(1 + \frac{r - c}{\tan^2 2\theta + c}\right), \tag{61}$$

where

$$r = \frac{2\mu}{\lambda_1 - \lambda_2}, \quad c = \frac{4\lambda_1\mu}{(\lambda_1 + \lambda_2 + 2\mu)(\lambda_1 - \lambda_2)}. \tag{62}$$

One sees that for $r > c$ or

$$\lambda_2 + 2\mu > \lambda_1, \tag{63}$$

the equilibrium domain structure corresponds to $\theta_{eq} = 0, \pi/2$, and

$$f(\theta)_{\max} = f(0) = 1/\lambda_1,$$

while in the opposite case $\theta_{\rm eq} = \pi/4, 3\pi/4$, and

$$f(\theta)_{\max} = f(\pi/4) = \frac{2}{\lambda_1 + \lambda_2 + 2\mu}. \tag{64}$$

Throughout the present paper, we use the data for the material constants of $BaTiO_3$ and $PbTiO_3$ from Refs. 12,20–23 and of $Pb(Zr_{0.5}Ti_{0.5})O_3$ from Ref. 12. We see that for BTO and PTO the condition of Eq. (63) is met and therefore the equilibrium 180° domain structure consists of stripes parallel (perpendicular) to the cubic axes, see Fig. 3(a), while the opposite inequality applies to PZT and the stripes make 45° with the cubic axes there, Fig. 3(b). For PTO this is in agreement with the experimental data of Refs. 24 and 25. For BTO, our conclusion coincides with that of Dvorak and Janovec[26] who defined the equilibrium orientation of the 180° domain walls in BTO far from the phase transition. These authors were surprised by their own conclusion about a very weak orientational dependence of the domain structure energy given that the experimental observations[27] showed a clearly preferable orientation, the same as suggested by the theory.

It follows from our results that the weak orientational dependence of the domain structure energy takes place in the sinusoidal regime too, and not only for BTO, but for all three perovskites we have made the numerical estimates for.

Indeed, from Eq. (60) one sees that the orientational dependence of the domain structure energy comes from the function $B_2(\theta)$. The maximum difference of values in Eq. (57)

for $B_2(\theta)$ can be used to characterize the anisotropy of the domain structure energy

$$\Delta B_2 = B_{2\max} - B_{2\min} = \frac{2}{3}q_{12}^2|f(0) - f(\pi/4)| = \frac{4}{3}\frac{q_{12}^2}{\lambda_1}\frac{|\lambda_1 - \lambda_2 - 2\mu|}{\lambda_1 + \lambda_2 + 2\mu}. \quad (65)$$

We found $\Delta B_2/B_2 \sim 4 \times 10^{-3}$ for BTO, much smaller anisotropy $\sim 3 \times 10^{-4}$ for PTO, and an even smaller one for PZT where $\Delta B_2/B_2 \sim 4 \times 10^{-5}$ (we have used the parameters listed in Ref. 28). Such a weak angular dependence of the domain structure energy with respect to the underlying crystal lattice is in accordance with the phase field results of Ref. 21, which showed domain walls mainly with thermodynamically favorable orientations, but also the domain wall with strong deviations from thermodynamically favorable orientations.

Comparing our conclusions with the results of atomic modeling, we begin with a paper on PZT,[29] where the authors studied PZT films of the same composition, as we do. They commented on the question of the orientation of the domain walls: "In the general cases, we find that the direction along which the stripe domains align is not certain. It may be the x or the y axis and may also have an angle with the x or y axis." This is in complete agreement with our results about the extremely weak dependence of the domain structure energy on the domain wall orientation in PZT. Lai *et al.*[30] have considered the same system and made a more definitive conclusion about the domain wall orientation indicating that they are perpendicular to the in-plane crystallographic axes. This is in disagreement with our conclusion, but given the extremely small anisotropy of the domain structure energy it can hardly be taken too seriously: it can well be within the error margin of the numerical method. More serious is a disagreement in the case of BTO: both in Refs. 31 and 32 it has been found that the stripes make 45° with the cubic axes in variance with our conclusion. In the case of Ref. 32 one could speculate that this is due to the system temperature being 10 K while we are considering a vicinity of the phase transition, but this speculation does not apply to Ref. 31, where a broad temperature interval is considered. It could be that the smallness of the domain energy anisotropy provides an explanation of the disagreement in this case as well. We are unaware about studies of the anisotropy of the domain structure energy by numerical methods.

VI. LOSS OF STABILITY OF A SINGLE DOMAIN STATE

It is convenient to study the loss of stability of the single domain state with respect to the formation of a domain structure using Eq. (56). With this, we mean the loss of stability with respect to arbitrarily small "polarization waves" so that the original single domain state may be, in principle, either stable or metastable. Specifically, in our case, when Eq. (29) is valid, this state is metastable.[6]

A solution of the equations

$$\partial\tilde{F}/\partial p = 0, \quad \partial\tilde{F}/\partial a = 0, \quad (66)$$

corresponding to a single domain state ($p \neq 0$, $a = 0$) is possible only if $A_1 < 0$ with $p_{\rm extr}^2 = -A_1/\widetilde{B}$, where the subscript stands for the "extremum." This extremum is a minimum (which is relative in our case) if

$$\partial^2\tilde{F}/\partial p^2 > 0, \quad \partial^2\tilde{F}/\partial a^2 > 0, \quad (67)$$

at the point $p = p_{\rm extr}$, $a = 0$ given that $\partial^2\tilde{F}/\partial p\partial a$ is evidently zero at this point. The first inequality in Eq. (67) is obviously valid for $A_1 < 0$, while the validity of the second is not immediately evident.

We find from Eq. (56)

$$4\left(\frac{\partial^2\tilde{F}}{\partial a^2}\right)_{a=0,\,p=p_{\rm extr}} = A_2 + 3B_1(\theta)p_{\rm extr}^2 = A_2 - 3A_1 - 3A_1(B_1(\theta) - \widetilde{B})/\widetilde{B}. \quad (68)$$

From the condition $(\partial^2\tilde{F}/\partial a^2)_{a=0,\,p=p_{\rm extr}} = 0$, we obtain the value of A corresponding to a loss of stability of the single domain state with respect to the appearance of a polarization wave with a given orientation, $A_{pw}(\theta)$. It is convenient to present it in the form

$$A_{pw}(\theta) = -\frac{6\pi d}{\varepsilon_b d + \epsilon_e l} + Gk^2 + \left(\frac{4\pi d}{\varepsilon_b d + \epsilon_e l} - 2Gk^2\right)\beta(\theta), \quad (69)$$

where

$$\beta(\theta) = \frac{q_{11}^2 - q_{12}^2 f\lambda_1}{\widetilde{B}\lambda_1 + 2\left(q_{11}^2 - q_{12}^2 f\lambda_1\right)}. \quad (70)$$

The last term in Eq. (69) is the result of the polarization-strain coupling while the first two present the prior case without this coupling[6,10]. According to Eq. (67), the corresponding single domain state will be (meta)stable at low temperatures such that $A < \min A_{pw}(\theta)$.

The actual loss of stability of the single domain state corresponds to the minimum of $A_{pw}(\theta)$. We have seen in Sec. V that in perovskites the angular dependencies are very weak and we can neglect it, putting $f\lambda_1 = 1$. Then

$$\beta = \frac{q_{11}^2 - q_{12}^2}{\widetilde{B}\lambda_1 + 2\left(q_{11}^2 - q_{12}^2\right)}. \quad (71)$$

Since in BTO, PTO, and PZT $q_{11}^2 > q_{12}^2$ (Ref. 28), the last term in Eq. (69) is *positive* and therefore the region of *meta*stability of the *single* domain state in these systems is *broader* than according to Refs. 10 and 6, in apparent accordance with Ref. 13. However, there are serious reservations. First of all, the effect is not very spectacular. Indeed, the factor β in the last term of Eq. (69) is always less than one half, $\beta < 1/2$, approaching that value when $q_{11}^2 - q_{12}^2 \to \infty$. Therefore,

$$A_{pw} < -\frac{4\pi d}{\varepsilon_b d + \epsilon_e l}, \quad (72)$$

where the right-hand side (r.h.s.) corresponds to a *very strong* strain coupling. Recall that $A = -4\pi d/(\varepsilon_b d + \epsilon_e l)$, or $A_1 = 0$, corresponds to what was calculated in several papers as a "*critical thickness of single-domain ferroelectricity*" $l_c^{\rm SD}$, Eq. (31).

To get the opposite limit of a *weak strain coupling* for $A_{pw}(0)$, we put $q_{11}^2 - q_{12}^2 = 0$ and neglect Gk^2, as Pertsev and Kohlstedt[13] did. We see that

$$-\frac{6\pi d}{\varepsilon_b d + \epsilon_e l} < A_{pw}(0) < -\frac{4\pi d}{\varepsilon_b d + \epsilon_e l}, \tag{73}$$

that is, because of accounting for the polarization-strain coupling the value of $A_{pw}(0)$ changes always by less than 1.5 times. In the usual situation when $\varepsilon_b d < \epsilon_e l$ this is also the interval of change of the thickness corresponding to the absolute loss of stability of the single domain state at a *fixed temperature*.

The above moderate, less than 50%, range of change is in striking disagreement with a statement by Pertsev and Kohlstedt[13] who claimed more than an order of magnitude change due to their nullifying the electrostrictive constants. They do not report the details of their procedure, but it is clear from the rest of the paper that their suggestion of putting the electrostrictive constants to zero implied changes in the coefficients of the LGD free energy that should have been renormalized by the misfit strains, while such renormalization was neglected there. Evidently, it has nothing to do with the effects of the polarization-strain coupling omitted in Refs. 6 and 10 since this renormalization is automatically taken into account there, while the effect of the misfit strain on LGD coefficients was apparently neglected in a gedanken exercise performed in Ref. 13.

Specifically, we find that for the perovskites BTO and PTO $\beta = 0.4$, while in PZT this parameter is 0.1 (i.e., four times smaller). We see that BTO and PTO are similar and very close to the limit $q_{11}^2 - q_{12}^2 \to \infty$, $\beta = 0.5$ (i.e., the point of loss of stability of single domain state is quite close in these materials to the "critical thickness of single-domain ferroelectricity"). The latter situation does not acquire, however, a practical importance because if one fixes the temperature and reduces the film thickness starting with monodomain ferroelectric state at low temperatures or large thicknesses, this state will give way to domains *before* the thickness determined by the limit of the single domain state stability is reached. The matter is that single domain state is metastable, it may have a large life time at low temperatures and large film thicknesses but this life time goes essentially to zero (to atomic times) when the above mentioned temperature or thickness are approached.

Importantly, it follows from Eq. (69) that if $q_{11}^2 < q_{12}^2$, the account for the inhomogeneous strains shrinks the region of metastability of the single domain state. This shows that, contrary to the claim by Pertsev and Kohlstedt, there is no general physical phenomenon such as the stabilization of a single domain state because of inhomogeneous strains accompanying the formation of domains. This may seem surprising because solids are known to "dislike" the inhomogeneous strains (free energy usually goes up). Moreover, the expectation of Pertsev and Kohlstedt is justified for a free-standing film, at least for elastically isotropic solid.[16] But it is not certain for a film on substrate considered both by them and in the present work. To explain the physical reason, we recall that the coupling with strain renormalizes the coefficients before fourth-order terms in the LGD free energy (this is separate from renormalization by the misfit strain), in our case we mean the coefficients before p^4 and p^2a^2 terms. Then, one has to take into account that the homogeneous strains in the plane of a substrate are not possible while the inhomogeneous ones are. Both the homogeneous and inhomogeneous polarizations create a homogeneous strain, but to a different extent see Eqs. (36) and (38), while inhomogeneous strains are created, of course, by the inhomogeneous polarization only. The out-of-plane and in-plane strains couple with the ferroelectric polarization P_z by electrostriction terms with different coefficients and the final result of renormalization of the coefficient of p^2a^2 term is due to several contributions and it is not clear upfront. It should be obtained by a consistent analysis, as it has been done above. No reason is seen to discard the possibility that the inequality $q_{11}^2 < q_{12}^2$ can be realized in some systems, and one cannot exclude, at least for the moment, the possibility of favoring the multidomain state by the polarization-strain coupling. Interestingly enough, this favoring may be very strong: According to Eq. (69), the increase of the region of absolute instability of single domain state becomes infinite when $q_{12}^2 - q_{11}^2$ tends to $\bar{B}\lambda_1/2$ from below.

The "phase diagrams" for the epitaxial FE films on a misfit substrate are plotted in Figs. 4 and 5. The boundaries of the paraelectric phase, domains, and metastable single domain region for the $BaTiO_3/SrRuO_3/SrTiO_3$ system are shown in the temperature-film thickness $(T - l)$ plane in Fig. 5. They are found from the conditions that we discussed above and write down here for a reference:

$$\begin{aligned} A(T_d) &= -2Gk^2 = -2G\left(\frac{4\pi^3}{\varepsilon_\perp G l^2}\right)^{1/2} \\ &= -2\left(\frac{4\pi^3 G}{\varepsilon_\perp}\right)^{1/2}\frac{1}{l_d}, \\ A\left(T_c^{\mathrm{SD}}\right) &= -\frac{4\pi d}{\epsilon_e l_c^{\mathrm{SD}}}, \\ A\left(T_{ms}^{\mathrm{SD}}\right) &= -\frac{6\pi d}{\epsilon_e l_{ms}^{\mathrm{SD}}}, \end{aligned} \tag{74}$$

where $d/2 = \lambda = 0.8$ Å, $\epsilon_e = 8.45$ for the $SrRuO_3$ electrode, $G = 0.3$ Å^2, and $\varepsilon_\perp$ is the dielectric constant [see its definition below Eq. (17)] in the plane of the FE film, which has been found from the Landau coefficients[5,6]. The arrows in Fig. 5 show the evolution of the state at either $T = \text{const}$ or $l = \text{const}$.

One should understand that in both illustrations it is implied that the corresponding critical points have physical values as solutions to the conditions (74), or, equivalently, Eqs. (28), (27), (30), and (31). Consider first the lowering of the temperature at a fixed thickness l (Fig. 4, top panel), where the paraphase transforms into the domain state below the temperature T_d that is smaller than the critical temperature of the bulk ferroelectric transition T_c. We see that the single domain (SD) state would be *metastable* at low temperatures $T < T_{ms}^{\mathrm{SD}}$ in the region overlapping with the domain state. Note that the T_{ms}^{SD} plotted in Fig. 5 is found without accounting for the strain coupling. The strain coupling then shifts the boundary of metastability toward the so-called critical temperature for a single domain state T_c^{SD} thus broadening the range of metastability of the SD state, as shown in Fig. 4.

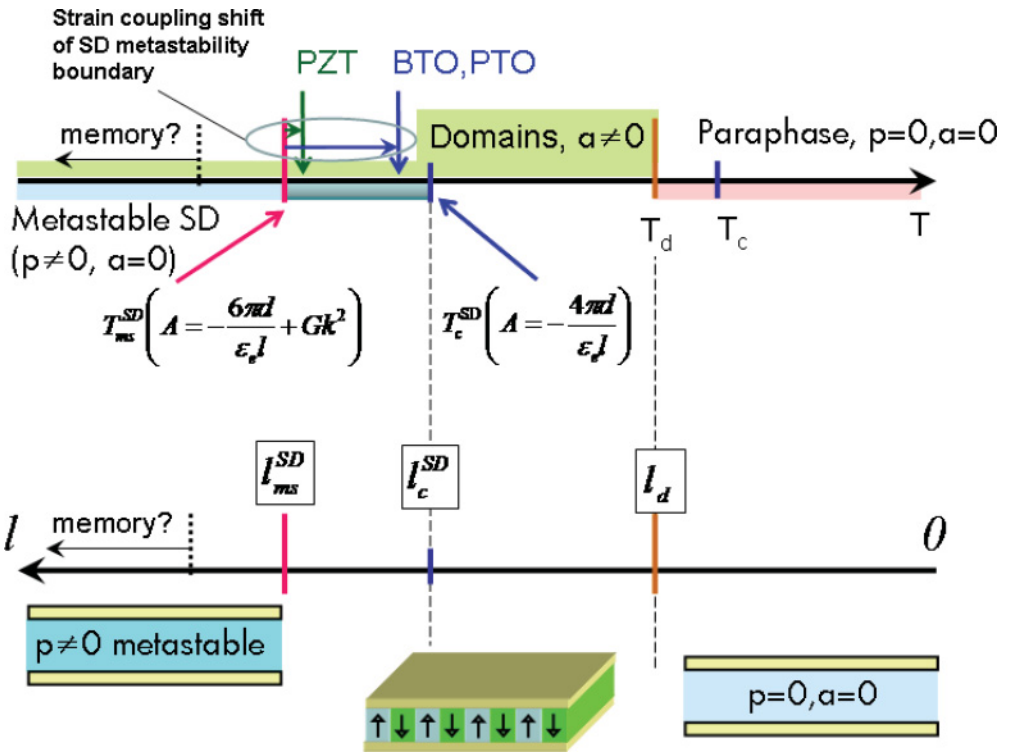

FIG. 4. (Color online) Regions of (meta)stability of the single domain and polydomain states in the ferroelectric film as a function of temperature T at fixed thickness (top) and as a function of the film thickness l at fixed T (bottom). Upon lowering the temperature at a fixed thickness l (top panel), the paraphase gives way to domains that are *stable* at all temperatures $T < T_d$, where T_d is below the critical temperature of the bulk ferroelectric transition T_c. The single domain (SD) state is *metastable* at low temperatures $T < T_{ms}^{\mathrm{SD}}$, when a strain coupling is neglected. The strain coupling shifts the boundary of metastability toward the so-called critical temperature for a single domain state, T_c^{SD}, as marked by the vertical arrows for the perovskites in question. The phase behavior of the films as a function of their thickness l at fixed temperature (bottom) is qualitatively similar. Very thin films are in a paraelectric phase that is replaced by domains at larger thicknesses $l > l_d$. The single domain state is metastable at thicknesses $l > l_{ms}^{\mathrm{SD}}$ and becomes suitable for memory applications at even larger (yet to be determined) thicknesses when the life time of the metastable state becomes sufficiently large. Strain coupling may extend the boundary of the metastability down to the so-called "critical thickness for SD ferroelectric state" l_c^{SD}.

The phase behavior of the films as a function of their thickness l at fixed temperature (Fig. 4, bottom panel) is qualitatively similar. Very thin films remain in a paraelectric phase that is replaced by the domains at larger thicknesses $l > l_d$. We see that both T_c^{SD} and l_c^{SD} are actually *unreachable* in the present case since the system may get to those points only by moving from the paraphase down (right to left on the phase diagram, Fig. 5), but such transitions are preempted by the domain instability that sets in first. The single domain state is metastable at thicknesses $l > l_{ms}^{\mathrm{SD}}$, and becomes suitable for *memory* applications at even larger (yet to be determined) thicknesses where its lifetime becomes sufficiently long.

VII. INSTABILITY OF THE CHECKERBOARD DOMAIN STRUCTURE

In the previous sections, we have assumed that the domain structure is stripe-like by taking into account only one "polarization wave." This and other possibilities have been studied by Chensky and Tarasenko[10] who considered the uniaxial ferroelectric isotropic in the x-y plane. Along with the stripe-like structure they discussed also the checkerboard

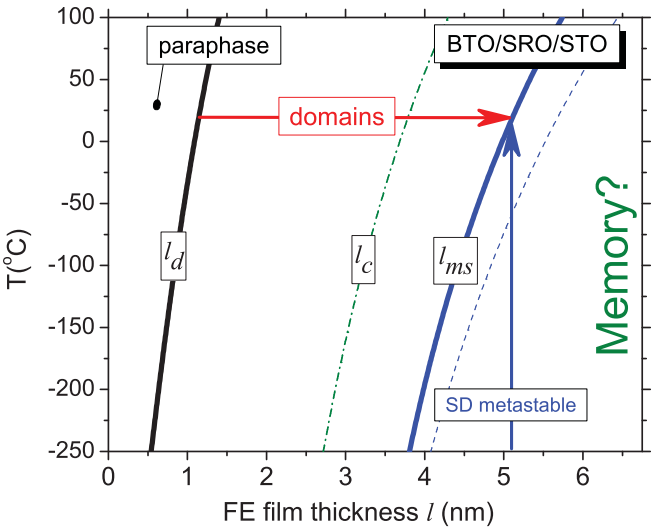

FIG. 5. (Color online) The phase diagram for $BaTiO_3/SrRuO_3/SrTiO_3$ films in the coordinates temperature thickness. The line marked l_d delineates the para- and domain phases, while the one marked l_{ms} indicates the boundary of the metastability regions of the single domain state.

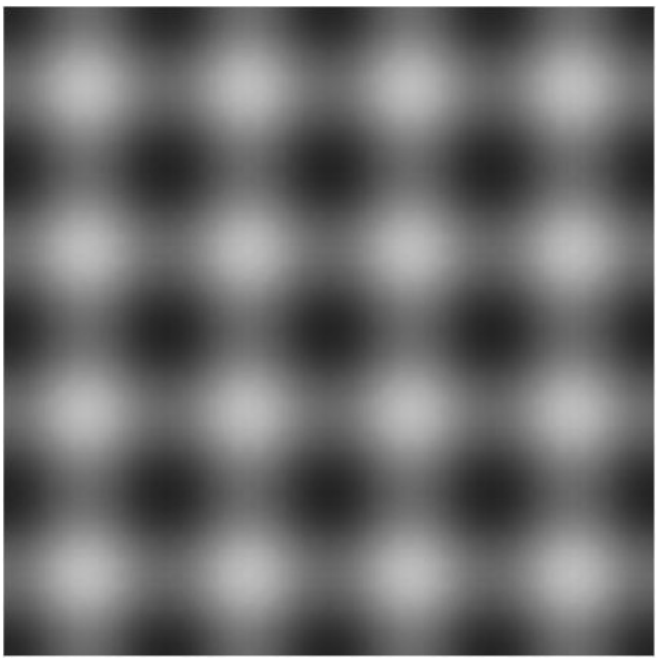

FIG. 6. Schematic of the checkerboard domain structure. It is absolutely unstable in case of $BaTiO_3$, $PbTiO_3$, and $Pb(Zr_{0.5}Ti_{0.5})O_3$ typical perovskite ferroelectrics.

and the hexagonal domain structures. The latter can be realized in the presence of an external field only, which is not a subject in this paper. However, a checkerboard structure should be analyzed as an alternative to the stripe structure. In Ref. 10, the authors stated that the checkerboard structure never realizes, although, surprisingly, there is no proof of this statement. In this section, we shall show that this structure is indeed unstable for the isotropic case treated in Ref. 10 and then show that this conclusion holds also when one explicitly takes into account the *polarization-strain interaction*, apart from mere renormalization of the LGD coefficients by the misfit strains.

Once again, we consider a short-circuited sample, that is, the ferroelectric polarization is described by

$$P_z = a_1 \cos \boldsymbol{k}_1 \boldsymbol{r} \cos qz + a_2 \cos \boldsymbol{k}_2 \boldsymbol{r} \cos qz, \tag{75}$$

where $\boldsymbol{k}_1$ and $\boldsymbol{k}_2$ are two noncollinear vectors whose modulus is given by Eq. (20) and whose (mutually orthogonal) directions remain unspecified for a moment, Fig. 6.

A. Checkerboard domains *without* elastic coupling ($q_{11} = q_{12} = 0$)

In this case the solution for the fields is [cf. Eq. (10)]

$$E_z = E_z^{k1} \cos \boldsymbol{k}_1 \boldsymbol{r} \cos qz + E_z^{k2} \cos \boldsymbol{k}_2 \boldsymbol{r} \cos qz, \tag{76}$$

$$E_{x,y} = E_{x,y}^{k1} \sin \boldsymbol{k}_1 \boldsymbol{r} \sin qz + E_{x,y}^{k2} \sin \boldsymbol{k}_2 \boldsymbol{r} \sin qz, \tag{77}$$

with Eq. (18) still applicable to spatial harmonics (as follows from the linearity of Maxwell equations) and the equation of state for the fundamental harmonics is the same as Eq. (12):

$$A_2 a_1 + \left[B P_z^3\right]_{\mathrm{cc}} = E_z^{k1}, \tag{78}$$

where one retains the terms $[B P_z^3]_{\mathrm{cc}} \propto \cos \boldsymbol{k}_1 \boldsymbol{r} \cos qz$ (symmetry dictates the analogous expressions for a_2). In the above equation,

$$\begin{aligned} P_z^3 &= (a_1 \cos \boldsymbol{k}_1 \boldsymbol{r} + a_2 \cos \boldsymbol{k}_2 \boldsymbol{r})^3 \cos^3 qz \\ &= \tfrac{9}{16}\left(a_1^3 + 2a_1 a_2^2\right) \cos \boldsymbol{k}_1 \boldsymbol{r} \cos qz + \tfrac{9}{16}\left(a_2^3 + 2a_2 a_1^2\right) \\ &\quad \times \cos \boldsymbol{k}_2 \boldsymbol{r} \cos qz + \cdots, \end{aligned} \tag{79}$$

so that we obtain for the fundamental harmonic the following equations of state:

$$A_2 a_1 + \frac{9B}{16}\left(a_1^3 + 2a_1 a_2^2\right) = 0, \tag{80}$$

and the analogous equation for a_2. Since these equations are obtained from the extremum of the free energy, $\partial \widetilde{F}/\partial a_{1(2)} = 0$, we again restore the full free energy, accounting for the symmetric contribution by the a_2 harmonic

$$V^{-1}\widetilde{F} = \frac{A_2}{8}(a_1^2 + a_2^2) + \frac{9}{256}B\left(a_1^4 + a_2^4\right) + \frac{9}{64}B a_1^2 a_2^2. \tag{81}$$

The equations of state have the checkerboard solution

$$a_1^2 = a_2^2 = -16A_2/27B. \tag{82}$$

Checking what type of extremum for the free energy is this solution

$$\frac{\partial^2 F}{\partial a_1^2} \times \frac{\partial^2 F}{\partial a_2^2} - \left(\frac{\partial^2 F}{\partial a_1 \partial a_2}\right)^2 = -\frac{1}{12}A_2^2 < 0,$$

we see that the checkerboard solution is the *maximum* of the free energy for some directions in the a_1,a_2 plane and is *absolutely unstable*.

B. Checkerboard domains *with* elastic coupling

We have seen above that the elastic coupling renormalizes the fourth order coefficients in formulas like Eq. (81) reducing them by some amounts that are different for different coefficients. Thus, instead of Eq. (81), we will have

$$V^{-1}\widetilde{F} = \frac{A_2}{8}\left(a_1^2 + a_2^2\right) + \frac{9}{256}\left(B_{21}a_1^4 + B_{22}a_2^4\right) + \frac{9}{64}B_3 a_1^2 a_2^2, \tag{83}$$

where B_{21} and B_{22} are given by Eq. (57) for the corresponding angles and B_3 is a new coefficient that depends on both angles and which can be, in principle, either positive or negative. Both from Eq. (57) and the cubic symmetry, one realizes that $B_{21} = B_{22} = B_2$. For what follows, it is important to mention that when B_3 is negative it cannot be of large absolute value, otherwise there will be directions in the (a_1,a_2) plane along which the free energy diminishes without limits at large values of a_1,a_2, meaning a global instability of the system. By putting $a_1 = a_2$, one sees from Eq. (83) that to avoid this instability the condition

$$B_2 + 2B_3 > 0, \tag{84}$$

should be fulfilled. Another obvious condition of the global stability is $B_2 > 0$.

The checkerboard solution is

$$a_1^2 = a_2^2 = \frac{-16A_2}{9(B_2 + 2B_3)}. \tag{85}$$

To analyze the stability of this solution, we calculate the second derivatives

$$\frac{\partial^2 F}{\partial a_1^2} = \frac{\partial^2 F}{\partial a_2^2} = \frac{A_2}{4} + \frac{27}{64}B_2 a_{1(2)}^2 + \frac{9}{32}B_3 a_{2(1)}^2 = -\frac{1}{2}A_2\frac{B_2}{B_2+2B_3},$$

$$\frac{\partial^2 F}{\partial a_1 \partial a_2} = \frac{9}{16}B_3 a_1 a_2 = \pm\frac{A_2 B_3}{B_2+2B_3},$$

then find the discriminant

$$Z \equiv \left(\frac{\partial^2 F}{\partial a_1^2}\right)\left(\frac{\partial^2 F}{\partial a_2^2}\right) - \left(\frac{\partial^2 F}{\partial a_1 \partial a_2}\right)^2 = \frac{1}{4}A_2^2\frac{B_2-2B_3}{B_2+2B_3}. \tag{86}$$

Our further study is aimed at finding out if and when the condition of positiveness of Z (i.e., $B_2 > 2B_3$) is compatible with the two conditions of the global stability mentioned above. Thus, we need formulas for the coefficients B_2 and B_3.

Turning to taking into account explicitly the polarization-strain coupling, we recall that in our approximation of sufficiently thick film the only source of the elastic strains is P_z^2. This function contains now a cross term stemming from

$$P_z^2 = (a_1 \cos \boldsymbol{k}_1\boldsymbol{r}\cos qz + a_2 \cos \boldsymbol{k}_2\boldsymbol{r}\cos qz)^2 \tag{87}$$

$$= \left[a_1^2 + a_2^2 + 2a_1a_2(\cos \boldsymbol{p}^+\boldsymbol{r} + \cos \boldsymbol{p}^-\boldsymbol{r}) + a_1^2\cos 2k_1 r + a_2^2\cos 2k_2 r\right]\frac{1+\cos 2qz}{4}, \tag{88}$$

where $\boldsymbol{p}^\pm = \boldsymbol{k}_1 \pm \boldsymbol{k}_2$. Naturally, the components of the strain tensor will have terms depending on $\cos \boldsymbol{p}^+\boldsymbol{r}$, $\cos \boldsymbol{p}^-\boldsymbol{r}$. We will have for u_{xx}

$$u_{xx} = u_{xx}^{(0)} + u_{xx}^{(1)}\cos 2qz + u_{xx}^{p+}\cos \boldsymbol{p}^+\boldsymbol{r} + u_{xx}^{p-}\cos \boldsymbol{p}^-\boldsymbol{r} + u_{xx}^{q+}\cos \boldsymbol{p}^+\boldsymbol{r}\cos 2qz + u_{xx}^{q-}\cos \boldsymbol{p}^-\boldsymbol{r}\cos 2qz + u_{1,xx}^{(3)}\cos 2k_1 r + u_{2,xx}^{(3)}\cos 2k_2 r + \left(u_{1,xx}^{(4)}\cos 2k_1 r + u_{2,xx}^{(4)}\cos 2k_2 r\right)\cos 2qz,$$

and the analogous equations for u_{yy} and u_{zz}.

From our previous experience, it becomes immediately clear that $u_{xx(yy)}^{p\pm} = u_{xx(yy)}^{q\pm}$ since the equations for those components do not depend on z and we can now drop the indices p and q from the corresponding terms, leaving only $u_{xx(yy)}^{+,-}$. Also, due to the same reason as above, $u_{xx(yy)}^{(0)} = u_{xx(yy)}^{(1)} = 0$ [cf. Eq. (39)]. Then, one can write

$$u_{xx} = (u_{xx}^+\cos \boldsymbol{p}^+\boldsymbol{r} + u_{xx}^-\cos \boldsymbol{p}^-\boldsymbol{r})(1+\cos 2qz) + u_{1,xx}^{(3)}\cos 2\boldsymbol{k}_1\boldsymbol{r} + u_{2,xx}^{(3)}\cos 2\boldsymbol{k}_2\boldsymbol{r} + \left(u_{1,xx}^{(4)}\cos 2\boldsymbol{k}_1\boldsymbol{r} + u_{2,xx}^{(4)}\cos 2\boldsymbol{k}_2\boldsymbol{r}\right)\cos 2qz,$$

and a similar equation for u_{yy}. The "diagonal" terms for the first (second) $\boldsymbol{k}_{1(2)}$ harmonic are

$$u_{1(2),xx}^{(3)} + u_{1(2),yy}^{(3)} = u_{1(2),xx}^{(4)} + u_{1(2),yy}^{(4)} = -q_{12}\frac{a_{1(2)}^2 f(\theta_{1(2)})}{4}.$$

All the cross terms satisfy

$$\lambda_1\frac{\partial^2 u_x^\pm}{\partial x^2} + (\lambda_2+\mu)\frac{\partial^2 u_y^\pm}{\partial y\partial x} + \mu\frac{\partial^2 u_x^\pm}{\partial y^2} + q_{12}\frac{\partial P_z^{2\pm}}{\partial x} = 0, \tag{89}$$

$$\lambda_1\frac{\partial^2 u_y^\pm}{\partial y^2} + (\lambda_2+\mu)\frac{\partial^2 u_x^\pm}{\partial y\partial x} + \mu\frac{\partial^2 u_y^\pm}{\partial x^2} + q_{12}\frac{\partial P_z^{2\pm}}{\partial y} = 0, \tag{90}$$

where $P_z^{2\pm} = \frac{1}{2}a_1a_2\cos \boldsymbol{p}^\pm\boldsymbol{r}$, in components $u_{x(y)}^\pm \propto \sin \boldsymbol{p}^\pm\boldsymbol{r}$, $\partial^2 u_i^\pm/\partial x^2 = -(p_x^\pm)^2 u_i^\pm$, and so on

$$\lambda_1 p_x^{\pm 2}u_x^\pm + (\lambda_2+\mu)p_x^\pm p_y^\pm u_y^\pm + \mu p_y^{\pm 2}u_x^\pm + q_{12}p_x^\pm\tfrac{1}{2}a_1a_2 = 0, \tag{91}$$

$$\lambda_1 p_y^{\pm 2}u_y^\pm + (\lambda_2+\mu)p_x^\pm p_y^\pm u_x^\pm + \mu p_x^{\pm 2}u_y^\pm + q_{12}p_y^\pm\tfrac{1}{2}a_1a_2 = 0. \tag{92}$$

Then,

$$u_{xx}^\pm + u_{yy}^\pm = p_x^\pm u_x^\pm + p_y^\pm u_y^\pm = -q_{12}\frac{a_1a_2}{2}f(\theta^\pm). \tag{93}$$

where the angle $\theta^\pm$ is defined analogously to θ from $p_x^\pm = p\cos\theta^\pm$ and $p_y^\pm = p\sin\theta^\pm$. For u_{zz}, we conclude, as above, that only $u_{zz}^{(0)}$ and $u_{zz}^{(1)}$ are nonzero and, following the same reasoning as for the stripe phase, we obtain

$$u_{zz}^{(0)} = u_{zz}^{(1)} = -\frac{q_{11}}{4\lambda_1}\left(a_1^2 + a_2^2\right).$$

Having solved the elastic problem, we are now in a position to write down the constituent equations containing a_1 and a_2 only. To this end, we write two equations for a_1 and a_2 analogous to Eq. (21) but this time $[\cdots]_{cc}$ would mean the proportionality to $\cos \boldsymbol{k}_1\boldsymbol{r}\cos qz$ or $\cos \boldsymbol{k}_2\boldsymbol{r}\cos qz$, respectively. Since both equations have the same structure, we will discuss that for a_1 only and, for the sake of brevity, we will mention only the terms containing a_2, the other terms are the same as for the one-sinusoid case discussed above.

For clarity sake, we repeat Eq. (21) with a minor change for the present case:

$$A_2a_1 + \left[BP_z^3 + 2q_{11}P_zu_{zz} + 2q_{12}P_z(u_{xx}+u_{yy})\right]_{cc} = 0. \tag{94}$$

It is straightforward to find that the a_2-containing term stemming from $[P_z^3]_{cc}$ is $9a_1a_2^2/8$. From Eq. (26), one sees that $[P_zu_{zz}]_{cc} = a_1(u_{zz}^{(0)} + \frac{1}{2}u_{zz}^{(1)})$, recall that now we consider the case $p = 0$, and the contribution of this term is

$$-\frac{3q_{11}}{8\lambda_1}a_1a_2^2.$$

Now,

$$[P_z(u_{xx}+u_{yy})]_{cc} = \frac{a_1}{2}\left(u_{1,xx}^{(3)} + u_{1,yy}^{(3)}\right) + \frac{a_1}{4}\left(u_{1,xx}^{(4)} + u_{1,yy}^{(4)}\right) + \frac{3}{4}a_2(u_{xx}^+ + u_{yy}^+ + u_{xx}^- + u_{yy}^-),$$

and the contribution of this term to the equation of state is

$$-q_{12}\frac{3a_1a_2}{8}[f(\theta^+) + f(\theta^-)].$$

Finally, the constituent equation for a_1 takes the form

$$A_2a_1 + \tfrac{9}{16}a_1^3B_2(\theta_1) + \tfrac{9}{8}a_1a_2^2B_3(\theta^+,\theta^-) = 0,$$

where we have introduced

$$B_3(\theta^+,\theta^-) = B - \frac{2}{3}\frac{q_{11}^2}{\lambda_1} - \frac{2}{3}q_{12}^2[f(\theta^+) + f(\theta^-)]. \quad (95)$$

Similarly to the case of one sinusoid, we recover the free energy

$$F = \frac{A_2}{8}\left(a_1^2 + a_2^2\right) + \frac{9}{256}B_2(\theta_1)a_1^4 + \frac{9}{256}B_2(\theta_2)a_2^4 + \frac{9}{64}B_3(\theta^+,\theta^-)a_1^2a_2^2. \quad (96)$$

Recall that the square symmetry suggests that $B_2(\theta_1) = B_2(\theta_2)$ and $B_2(\theta)$ is given by Eq. (57).

Turning to examining the sign of the discriminant Z, we should mention that according to Eqs. (57) and (95)

$$B_2 - 2B_3 = -B + \tfrac{4}{3}q_{12}^2\left[f(\theta^+) + f(\theta^-) - \tfrac{1}{2}f(\theta_1)\right].$$

One sees that the maxima of Z correspond to the maxima of $f(\theta^+)$ and $f(\theta^-)$ [note that $f(\theta^+_{\max}) = f(\theta^-_{\max})$ because of the cubic symmetry], which are, automatically, the minima of $f(\theta_1)$ as we have seen in Sec. V [since the corresponding angles are different by $\pi/4$]. Then,

$$[B_2 - 2B_3]_{\max} = -B + \tfrac{4}{3}q_{12}^2\left[2f(\theta_{\max}) - \tfrac{1}{2}f(\theta_{\min})\right].$$

Using the values of $f(\theta_{\max})$ and $f(\theta_{\min})$ found in Sec. V, we find that if $\lambda_2 + 2\mu > \lambda_1$,

$$[B_2 - 2B_3]_{\max} = -B + \frac{4}{3}q_{12}^2\left(\frac{2}{\lambda_1} - \frac{1}{\lambda_1+\lambda_2+2\mu}\right) = -B + \frac{4}{3}q_{12}^2\frac{2(\lambda_2+2\mu)+\lambda_1}{\lambda_1(\lambda_1+\lambda_2+2\mu)}, \quad (97)$$

and if $\lambda_2 + 2\mu < \lambda_1$,

$$[B_2 - 2B_3]_{\max} = -B + \frac{4}{3}q_{12}^2\left(\frac{4}{\lambda_1+\lambda_2+2\mu} - \frac{1}{2\lambda_1}\right) = -B + \frac{4}{3}q_{12}^2\frac{7\lambda_1-\lambda_2-2\mu}{2\lambda_1(\lambda_1+\lambda_2+2\mu)}. \quad (98)$$

To prove that the checkerboard structure can be stable, at least in principle, with respect to small fluctuations, we should demonstrate that the positiveness of $[B_2 - 2B_3]_{\max}$ is compatible with the conditions $B_2 > 0$ and $[B_2 - 2B_3]_{\min} > 0$ which guarantee the global stability of the system. We do not intend to perform an exhaustive analysis, but want only to demonstrate that this is possible under certain conditions, unlike in the case without the elastic coupling. As an example, we consider a system with a weak elastic anisotropy, which is valid for the perovskites (i.e., we shall assume $\lambda_2 + 2\mu \simeq \lambda_1$, and $q_{11} = 0$). Both Eqs. (97) and (98) then give

$$[B_2 - 2B_3]_{\max} \simeq -B + \frac{2q_{12}^2}{\lambda_1}, \quad (99)$$

and give for the positiveness of $[B_2 - 2B_3]_{\max}$ the same condition $q_{12}^2 > B\lambda_1/2$, while the condition $B_2 > 0$ now reads $q_{12}^2 < 3B\lambda_1/2$. One sees that for a nearly elastically isotropic ferroelectric with $q_{11} = 0$, the checkerboard structure is at least metastable if

$$3B\lambda_1/2 > q_{12}^2 > B\lambda_1/2.$$

Of course, the above set of the material coefficients looks fairly exotic, but it is just an example aimed at nothing more but a demonstration that the checkerboard domain structures are allowed due to the elastic coupling when certain conditions on the material coefficients are met.

In the case of real perovskite films the checkerboard structure is not stable. To see this, we can rewrite Eq. (99) in the form

$$[B_2 - 2B_3]_{\max} \simeq -\widetilde{B} - \frac{2}{\lambda_1}\left(q_{11}^2 - q_{12}^2\right) < 0.$$

Indeed, we have already mentioned above that for the perovskites $q_{11}^2 > q_{12}^2$, while $\widetilde{B} > 0$ there. Therefore, in the perovskites the checkerboard domain structure is absolutely *unstable*.

VIII. CONCLUSION

With the use of the Landau-Ginzburg-Devonshire theory, we have studied the effects of polarization-strain coupling when defining the character of equilibrium domain structures and the limits of absolute instability of a single domain state in thin films of cubic ferroelectric films on a misfit substrate. On the compressive substrate, the cubic ferroelectric behaves substantially as a uniaxial ferroelectric with the polar axis perpendicular to the film. The film is sandwiched between the electrodes that do not provide a perfect screening of the depolarizing field because of the finite Thomas-Fermi screening length. Such a system is exemplified by the (100) $BaTiO_3/SrRuO_3/SrTiO_3$ film and similar perovskite structures. Quantitative results have been obtained for $BaTiO_3$, $PbTiO_3$, and $Pb(Zr_{0.5}Ti_{0.5})O_3$. We have found that close to the paraelectric-ferroelectric phase transition or at the film thicknesses close to the minimal thickness compatible with the ferroelectricity, the equilibrium domain structure in perovskites is the stripe-wise one with the stripes parallel (perpendicular) to the cubic axes in $BaTiO_3$, $PbTiO_3$, while running at 45° to the cubic axes in $Pb(Zr_{0.5}Ti_{0.5})O_3$. The energy of the domain structure depends very weakly on the stripe orientation, the maximum change proves to be well below 1% in all three cases. We found that because of the polarization-strain coupling a competing checkerboard domain structure may, at least in principle, be an equilibrium or a metastable one when certain conditions on the material constants are met, but we are not aware of any material system where such conditions are met. The limit of absolute instability of the single domain state changes due to the polarization-strain coupling. Thus, the interval where the absolute instability is absent, meaning a metastability in the cases at hand, widens in perovskites in agreement with the earlier conclusion by Pertsev and Kohlstedt.[13] However, this effect is much smaller than that claimed by them. The increase of the metastability range is substantial in $BaTiO_3$ and $PbTiO_3$, where the absolute instability limit becomes close to what is often called the "critical thickness for ferroelectricity" l_c^{SD}, Fig. 5, but without accounting for the domain formation. The effect is much smaller in $Pb(Zr_{0.5}Ti_{0.5})O_3$. We have found also

that the polarization-strain coupling can lead to the narrowing of the region of relative stability of the single domain state under certain conditions on the material constants, but we are not aware of an experimental realization of these conditions.

ACKNOWLEDGMENT

APL has been partly supported by the Ministry of Science and Education of Russian Federation (State Contract No. 02.740.11.5156).

[1] D. J. Kim, J. Y. Jo, Y. S. Kim, Y. J. Chang, J. S. Lee, J.-G. Yoon, T. K. Song, and T. W. Noh, Phys. Rev. Lett. **95**, 237602 (2005).

[2] Y. S. Kim, D. H. Kim, J. D. Kim, Y. J. Chang, T. W. Noh, J. H. Kong, K. Char, Y. D. Park, S. D. Bu, J.-G. Yoon, and J.-S. Chung, Appl. Phys. Lett. **86**, 102907 (2005).

[3] Y. S. Kim, J. Y. Jo, D. J. Kim, Y. J. Chang, J. H. Lee, T. W. Noh, T. K. Song, J.-G. Yoon, J.-S. Chung, S. I. Baik, Y.-W. Kim, and C. U. Jung, Appl. Phys. Lett. **88**, 072909 (2006).

[4] J. Junquera and P. Ghosez, Nature (London) **422**, 506 (2003).

[5] A. M. Bratkovsky and A. P. Levanyuk, Appl. Phys. Lett. **89**, 253108 (2006).

[6] A. M. Bratkovsky and A. P. Levanyuk, J. Comput. Theor. Nanosci. **6**, 465 (2009).

[7] G. B. Stephenson and K. R. Elder, J. Appl. Phys. **100**, 051601 (2006).

[8] H. Suhl, Appl. Phys. **8**, 217 (1975).

[9] H. Schmidt and F. Schwabl, Z. Phys. B **30**, 197 (1978); F. Fishman, F. Schwabl, and D. Schwenk, Phys. Lett. A **121**, 192 (1987).

[10] E. V. Chensky and V. V. Tarasenko, Sov. Phys. JETP **56**, 618 (1982) [Zh. Eksp. Teor. Fiz. **83**, 1089 (1982)].

[11] P. Aguado-Puente and J. Junquera, Phys. Rev. Lett. **100**, 177601 (2008).

[12] N. A. Pertsev and H. Kohlstedt, e-print arXiv:cond-mat/0603762 (2006).

[13] N. A. Pertsev and H. Kohlstedt, Phys. Rev. Lett. **98**, 257603 (2007).

[14] N. A. Pertsev and H. Kohlstedt, Phys. Rev. Lett. **100**, 149702 (2008).

[15] A. M. Bratkovsky and A. P. Levanyuk, Phys. Rev. Lett. **100**, 149701 (2008).

[16] A. M. Bratkovsky and A. P. Levanyuk, Philos. Mag. **90**, 113 (2010).

[17] A. K. Tagantsev and G. Gerra, J. Appl. Phys. **100**, 051607 (2006).

[18] S. P. Timoshenko and J. N. Goodier, *Theory of Elasticity*, 3rd ed., (McGraw-Hill, New York, 1970).

[19] A. G. Khachaturyan, *Theory of Structural Phase Transformations in Solids* (John Wiley, New York, 1983), p. 370.

[20] N. A. Pertsev, A. G. Zembilgotov, and A. K. Tagantsev, Phys. Rev. Lett. **80**, 1988 (1998).

[21] Y. Li, S. Y. Hu, Z. K. Liu, and L. Q. Chen, Acta Mater. **50**, 395 (2002).

[22] G. Sheng, J. X. Zhang, Y. L. Li, S. Choudhury, Q. X. Jia, Z. K. Liu, and L. Q. Chen, J. Appl. Phys. **104**, 054105 (2008).

[23] J. Hlinka, Ferroelectrics **375**, 132 (2008); J. Hlinka and P. Márton, Phys. Rev. B **74**, 104104 (2006); P. Marton, I. Rychetsky, and J. Hlinka, *ibid.* **81**, 144125 (2010).

[24] S. K. Streiffer, J. A. Eastman, D. D. Fong, C. Thompson, A. Munkholm, M. V. Ramana Murty, O. Auciello, G.-R. Bai, and G. B. Stephenson, Phys. Rev. Lett. **89**, 067601 (2002).

[25] D. D. Fong, G. B. Stephenson, S. K. Streiffer, J. A. Eastman, O. Auciello, P. H. Fuoss, and C. Thompson, Science **304**, 1650 (2004).

[26] V. Dvorak and V. Janovec, Jpn. J. Appl. Phys. **4**, 400 (1965).

[27] J. Fousek and M. Safrankova, Jpn. J. Appl. Phys. **4**, 403 (1965).

[28] In cubic crystals the usual notations for the elastic constants are $\lambda_1 = c_{11}, \lambda_2 = c_{12}$, and $\mu = c_{44}$. We have used the following values of the parameters in the SI units: (i) for $BaTiO_3$ (Refs. 12 and 20); $c_{11} = 1.755 \times 10^{11}$ Nm^{-2}, $c_{12} = 8.464 \times 10^{10}$ Nm^{-2}, $c_{44} = 1.082 \times 10^{11}$ Nm^{-2}, $q_{11} = 1.203 \times 10^{10}$ JmC^{-2}, $q_{12} = -1.878 \times 10^{9}$ JmC^{-2}, $\tilde{B} = 3.6 \times 10^{8}$ Jm^5C^{-4}; $G = 0.3$ $Å^2$ (Refs. 5 and 6, cf. Ref. 23); (ii) for $PbTiO_3$ (Ref. 21): $c_{11} = 1.746 \times 10^{11}$ Nm^{-2}, $c_{12} = 7.937 \times 10^{10}$ Nm^{-2}, $c_{44} = 1.111 \times 10^{11}$ Nm^{-2}, $q_{11} = 1.141 \times 10^{10}$ JmC^{-2}, $q_{12} = 4.607 \times 10^{8}$ JmC^{-2}, $\tilde{B} = 2.0 \times 10^{8}$ Jm^5C^{-4}; (iii) for $Pb(Zr_{0.5}Ti_{0.5})O_3$ (Ref. 12): $c_{11} = 1.545 \times 10^{11}$ Nm^{-2}, $c_{12} = 8.405 \times 10^{10}$ Nm^{-2}, $c_{44} = 3.484 \times 10^{10}$ Nm^{-2}, $q_{11} = 7.189 \times 10^{9}$ JmC^{-2}, $q_{12} = -2.853 \times 10^{9}$ JmC^{-2}, $\tilde{B} = 1.43 \times 10^{9}$ Jm^5C^{-4}.

[29] Z. Wu, N. Huang, Z. Liu, J. Wu, W. Duan, B.-L. Gu, and X.-W. Zhang, Phys. Rev. B **70**, 104108 (2004).

[30] B.-K. Lai, I. Ponomareva, I. I. Naumov, I. A. Kornev, H. Fu, L. Bellaiche, and G. J. Salamo, Phys. Rev. Lett. **96**, 137602 (2006).

[31] S. Tinte and M. G. Stachiotti, Phys. Rev. B **64**, 235403 (2001).

[32] B.-K. Lai, I. Ponomareva, I. A. Kornev, L. Bellaiche, and G. J. Salamo, Phys. Rev. B **75**, 085412 (2007).